THE JOURNAL OF BIOLOGICAL CHEMISTRY VOL. 285, NO. 10, pp. 7430–7439, March 5, 2010

Zinc-induced Neurotoxicity Mediated by Transient Receptor Potential Melastatin 7 Channels*[S]

Received for publication, July 2, 2009, and in revised form, December 24, 2009 Published, JBC Papers in Press, January 4, 2010, DOI 10.1074/jbc.M109.040485

Koichi Inoue, Deborah Branigan, and Zhi-Gang Xiong[1]

From the Robert S. Dow Neurobiology Laboratories, Legacy Research, Portland, Oregon 97232

Transient receptor potential melastatin 7 (TRPM7) channels are novel Ca^{2+}-permeable non-selective cation channels ubiquitously expressed. Activation of TRPM7 channels has been shown to be involved in cellular Mg^{2+} homeostasis, diseases caused by abnormal magnesium absorption, and in Ca^{2+}-mediated neuronal injury under ischemic conditions. Here we show strong evidence suggesting that TRPM7 channels also play an important role in cellular Zn^{2+} homeostasis and in Zn^{2+}-mediated neuronal injury. Using a combination of fluorescent Zn^{2+} imaging, small interfering RNA, pharmacological analysis, and cell injury assays, we show that activation of TRPM7 channels augmented Zn^{2+}-induced injury of cultured mouse cortical neurons. The Zn^{2+}-mediated neurotoxicity was inhibited by nonspecific TRPM7 blockers Gd^{3+} or 2-aminoethoxydiphenyl borate, and by knockdown of TRPM7 channels with small interfering RNA. In addition, Zn^{2+}-mediated neuronal injury under oxygen-glucose deprivation conditions was also diminished by silencing TRPM7. Furthermore, we show that overexpression of TRPM7 channels in HEK293 cells increased intracellular Zn^{2+} accumulation and Zn^{2+}-induced cell injury, while silencing TRPM7 by small interfering RNA attenuated the Zn^{2+}-mediated cell toxicity. Thus, TRPM7 channels may represent a novel target for neurological disorders where Zn^{2+} toxicity plays an important role.

Calcium toxicity is one of the key factors responsible for neuronal cell death associated with neurological disorders (1). Following brain ischemia, for example, intracellular calcium concentration ($[Ca^{2+}]_i$)[2] increases dramatically, either through extracellular calcium entry or intracellular calcium release. Excessive elevation of $[Ca^{2+}]_i$ activates destructive signaling cascades leading to neuronal cell death.

Despite a number of studies that have clearly demonstrated the role of Ca^{2+} toxicity in ischemic neuronal death, clinical trials targeting the Ca^{2+} entry pathways, *e.g.* by using glutamate antagonists, have had inconclusive results (2, 3). Although the importance of $[Ca^{2+}]_i$ accumulation in neuronal cell death cannot be denied, certain results with $[Ca^{2+}]_i$ measurement have been questionable. For example, previous studies reported that some indicators commonly used for calcium imaging, *e.g.* Calcium Green-1 and fura-2, are responsive to zinc with an extremely high affinity, and that specific zinc chelators reduced the intensity of calcium indicators (4–7). These findings suggest that some of the biological effects previously assumed to be mediated by Ca^{2+} may be mediated, at least partially, by zinc ions. Like calcium, recent studies have demonstrated that zinc ions play an important role in neuronal injuries associated with various neurological conditions (8, 9). The exact pathways mediating intracellular zinc accumulations and toxicity are, however, not clear.

Zinc is one of the most crucial trace metals in cells. For example, zinc is required for the function of a broad range of enzymes involved in transcription, protein synthesis, and signal transductions (10). Although there are low levels of free zinc in cells, most zinc ions are bound to intracellular proteins (11). The mechanisms that affect the free zinc concentration are, therefore, pivotal for maintaining normal brain function. Although the extracellular fluid may contain up to several micromolar of zinc, intracellular zinc concentration ($[Zn^{2+}]_i$) is generally maintained at 10^{-9}–10^{-10} M (10, 12, 13). This steep gradient across the cell membrane is maintained primarily by zinc extrusion systems such as zinc transporters (ZnTs). At least 10 members of ZnTs, with different tissue distribution, have been identified in the ZnTs family. They promote the efflux of intracellular zinc into extracellular space or uptake of zinc into vesicles (14, 15). In contrast to ZnTs, Zrt- and Irt-like proteins, or ZIPs, are known to transport zinc into the cells (14, 15). In addition, some calcium channels, *e.g.* voltage-dependent calcium channels (VDCCs), *N*-methyl-D-aspartate (NMDA) receptors, and amino-3-hydroxy-5-methyl-4-isoxazol propionate (AMPA)/kinate receptors have been reported to be zinc permeable (16, 17). The activities of these channels thus affect intracellular zinc homeostasis and toxicity. Unfortunately, clinical trials using the antagonists of these channels failed to provide satisfactory neuroprotection (2, 3).

Transient receptor potential melastatin 7 (TRPM7) is a member of the large TRP channel superfamily expressed in

* This work was supported, in whole or in part, by National Institutes of Health Grants R01NS47506 and R01NS49470 and American Heart Association Grant 0840132N.

[S] The on-line version of this article (available at http://www.jbc.org) contains supplemental Figs. S1–S3.

[1] To whom correspondence should be addressed: 1225 NE 2nd Ave., Portland, OR 97232. Tel.: 503-413-2086; Fax: 503-413-5465; E-mail: zxiong@Downeurobiology.org.

[2] The abbreviations used are: $[Ca^{2+}]_i$, intracellular calcium concentration; $[Zn^{2+}]_i$, intracellular zinc concentration; ZnT, zinc transporter; TRP, transient receptor potential; TRPM7, TRP melastatin 7; VDCCs, voltage-dependent calcium channels; NMDA, *N*-methyl-D-aspartate; AMPA, amino-3-hydroxy-5-methyl-4-isoxazol propionate; HEK, human embryonic kidney; HEK:TRPM7 cells, HEK293 cells with inducible expression of TRPM7 channels; shRNA, short hairpin RNA; eGFP, enhanced green fluorescence protein; LDH, lactate dehydrogenase; ECF, extracellular fluid; OGD, oxygen-glucose deprivation; PI, propidium iodide; TPEN, *N*,*N*,*N*′,*N*′-tetrakis-(2-pyridylmethyl)ethylenediamine; TRPM7(−) cells, HEK:TRPM7 cells without induced expression of TRPM7 channels; TRPM7(+) cells, HEK:TRPM7 cells with induced expression of TRPM7 channels; MRE, metal regulatory element; $[Ca^{2+}]_o$, extracellular calcium concentration.

almost every tissue and cell type (18–20). Increasing evidence suggests that activation of TRPM7 channels contributes to various physiological and pathophysiological processes (21–23). Notably, we demonstrated that activation of TRPM7 channels by oxygen-free radicals plays a critical role in hypoxia-induced, glutamate-independent, neuronal injury (24). In addition to well established Ca^{2+} permeability, TRPM7 is, at present, the only known zinc permeable channel among the TRP family of ion channels (18, 25). It is reported that zinc permeability for TRPM7 channels is 4-fold higher than Ca^{2+} (25). Despite these facts, it has not been established whether TRPM7 channels play a role in intracellular zinc dynamics at physiological/pathological relevant concentrations, and more importantly, in zinc-mediated neurotoxicity. Using a combination of fluorescent zinc imaging, metal response element-based reporter gene assay, cell injury analysis, and small interfering RNA techniques, we show strong evidence suggesting that TRPM7 channels represent a novel pathway for intracellular zinc accumulation and zinc-mediated neurotoxicity.

EXPERIMENTAL PROCEDURES

Cell Culture—Mouse cortical neurons were cultured as described previously (26). The protocol for the use of mice for neuronal cultures was reviewed and approved by the Institutional Animal Care and Use Committee of Legacy Clinical Research and Technology Center. Briefly, time-pregnant (embryonic day 16) Swiss mice (Charles River Laboratories) were anesthetized with halothane followed by cervical dislocation. Brains of fetuses were removed rapidly and placed in Ca^{2+}/Mg^{2+}-free cold phosphate-buffered saline. Cerebral cortices were dissected under a dissection microscope and incubated with 0.05% trypsin-EDTA for 10 min at 37 °C, followed by trituration with fire-polished glass pipettes. Cells were counted and plated in poly-L-ornithine-coated culture dishes or 24-well plates at a density of 1×10^6 cells/dish or 2×10^5 cells/well, respectively. Neurons were cultured with Neurobasal medium supplemented with B-27 (Invitrogen), and maintained at 37 °C in a humidified 5% CO_2 atmosphere incubator. Cultures were fed twice a week. Neurons were used for the experiments between days 11 and 15 *in vitro*.

Human embryonic kidney (HEK293) cells, with inducible expression of human TRPM7 channels (HEK:TRPM7 cells), were cultured in minimal essential medium supplemented with 10% fetal bovine serum and antibiotics (19). For the induction of TRPM7, the cells were treated with 1 μg/ml of tetracycline, as described in our previous studies (22).

Immunoblotting—Immunoblotting was performed as described previously (27). Cells cultured in 35-mm dishes or 6-well plates were lysed in lysis buffer (50 mM Tris-HCl, pH 7.5, 100 mM NaCl, 1% Triton X-100, and protease inhibitors (Roche Diagnostics)). After centrifugation at 12,000 $\times$ *g* at 4 °C for 30 min the lysates were collected. The aliquots were then mixed with Laemmli sample buffer and incubated at 37 °C for 1 h. The samples were resolved by 7.5% SDS-PAGE, followed by electrotransfer to polyvinylidene difluoride membranes. For visualization, blots were probed with antibodies against TRPM7 (1:250; Abgent) or β-actin (1:2000; Abcam), and detected using horseradish peroxidase-conjugated secondary antibodies (1:1000; Cell Signaling) and an ECL kit (GE Healthcare). The intensity of the protein band was densitometrically quantified.

Plasmid Construction and Transfection—The plasmid containing short hairpin RNA (shRNA) for silencing human TRPM7 was described previously (22).

To construct the plasmid for silencing mouse TRPM7, two oligonucleotides were annealed and inserted into pSilencer 1.0-U6 (Ambion) according to manufacturer's instructions. The target sequence for TRPM7 corresponded to coding region 5152–5172 (GenBank accession number NM021450 (28)). A fragment cut with BamHI was excised and inserted into the BamHI site of pCAGGS-eGFP (kindly provided by Dr. J. Miyazaki, Division of Stem Cell Regulation Research, Osaka University Medical School, Osaka, Japan) to express both enhanced green fluorescence protein (eGFP) and shRNA (TRPM7-shRNA/eGFP) (29). For the negative control, a fragment cut with BamHI from pSilencer 1.0-U6 was inserted into pCAGGS-eGFP (control/eGFP).

For transfection, FuGENE HD (Roche Diagnostics) and NeuroFect (Genlantis) were used for HEK:TRPM7 cells, and for cortical neurons (between days 8 and 11 *in vitro*) in accordance with the manufacturer's instructions. The transfection efficiencies, as determined by eGFP-positive cells, were 2–5% for cultured mouse cortical neurons.

Lactate Dehydrogenase (LDH) Assay—LDH measurement was performed as described in our previous studies (30, 31). Cells grown on 24-well plates were first washed with phosphate-buffered saline. 50 μl of the culture medium was taken from each well and placed into a 96-well plate for background LDH measurement. Cells were then treated with zinc containing medium for 1 or 2 h, followed by a wash and incubation in normal culture medium for 23 or 22 h, respectively. 50 μl of the medium was transferred from each well to 96-well plates for measurement of injury-mediated LDH release. For measurement of the maximal releasable LDH, cells were incubated with Triton X-100 (final concentration 0.5%) for 30 min at the end of each experiment. 50 μl of assay reagent from the cytotoxicity detection kit (Roche Diagnostics) was added to each sample according to the manufacturer's instructions. 30 min later, the absorbance at 492 and 620 nm was examined by a spectrometer (SpectraMax Plus, Molecular Devices). The values of the absorbance at 492 nm were subtracted by those at 620 nm to yield the value of LDH release.

Reporter Gene Assays—Cells grown on 24-well plates were transfected with p$(MREa)_6$-Luc (kindly provided by Dr. C. Seguin, Centre de Recherche en Cancerologie de l'Universite Laval) together with pRL-TK (Promega) to measure transfection efficiency (32). Expression plasmids were transfected in the following amounts per well: 0.3 μg of p$(MREa)_6$-Luc and 0.1 μg of pLR-TK for HEK:TRPM7 cells; 0.8 μg of shRNA-containing pCAGGS-eGFP, 0.9 μg of p$(MREa)_6$-Luc, and 0.3 μg of pLR-TK for cortical neurons. Luciferase assays were performed using the Dual-Luciferase Reporter System (Promega) with a microplate luminometer (Veritas™, Turner Biosystems), in which relative firefly luciferase activity was calculated by normalizing the transfection efficiency according *Renilla* luciferase activity. Relative firefly luciferase activity detected in the cell lysates was presented (33).

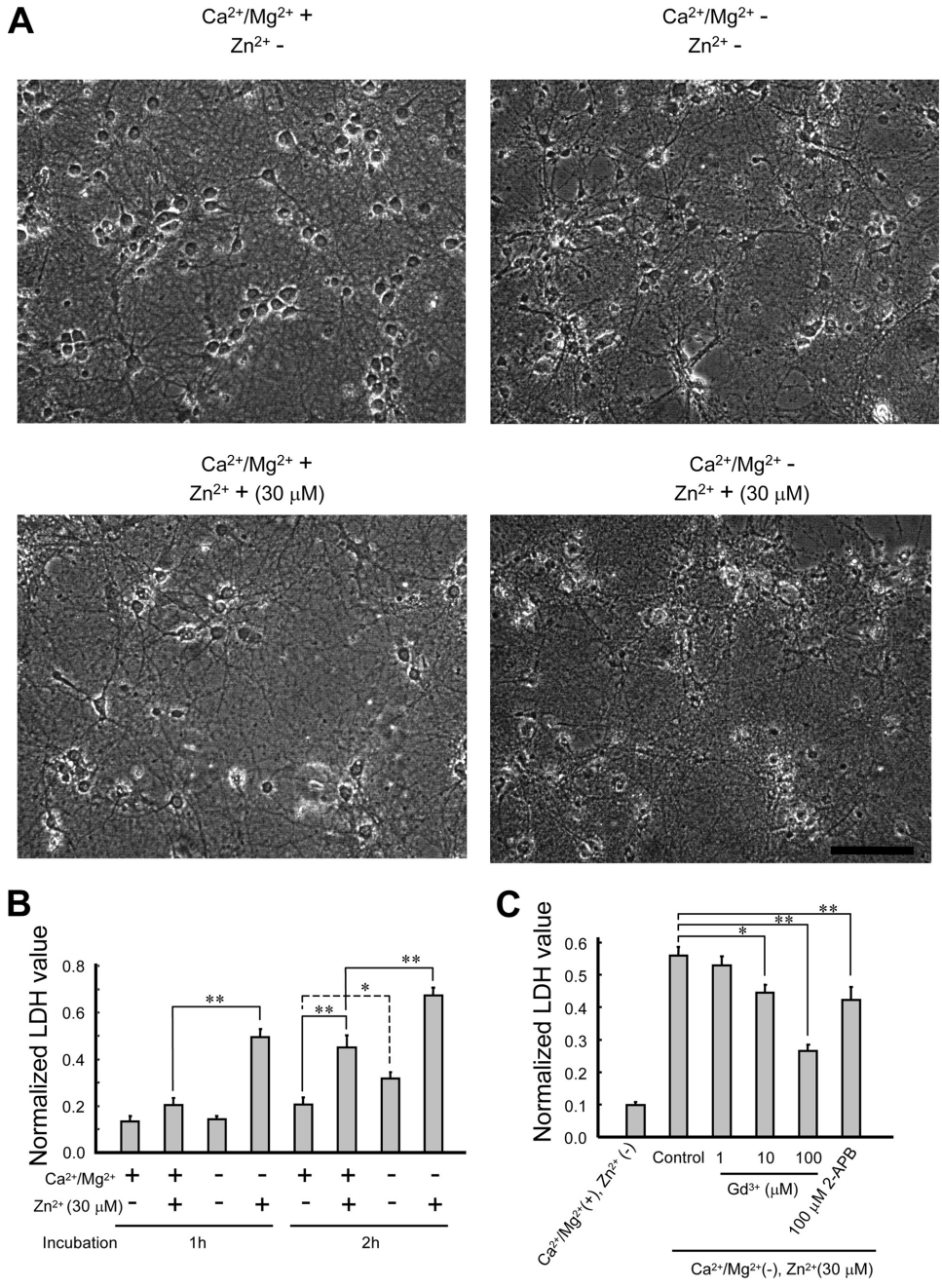

FIGURE 1. **Activation of TRPM7 channels by Ca^{2+}/Mg^{2+} removal exacerbates zinc toxicity in mouse cortical neurons.** *A*, representative phase-contrast images showing cultured mouse cortical neurons taken at 23 h following a 1-h treatment with the indicated solutions. *Scale bar*, 100 μm. *B*, relative LDH release induced by different treatments as indicated. Cells were incubated in different ECF for either 1 or 2 h, and then incubated with normal culture medium for 23 or 22 h, respectively. LDH samples were then taken and normalized to the maximal values. $n = 9–12$. *C*, inhibition of TRPM7 channels by Gd^{3+} or 2-aminoethoxydiphenyl borate (*2-APB*) reduced zinc toxicity. Cells were treated with the indicated condition for 1 h in the presence of different concentrations of Gd^{3+} or 100 μM 2-aminoethoxydiphenyl borate. Cells were then incubated with normal culture medium for 23 h, followed by LDH release assay ($n = 8–15$). *, $p < 0.05$; **, $p < 0.01$.

Zinc Imaging—The intracellular zinc level of HEK:TRPM7 cells or mouse cortical neurons was imaged using a zinc-sensitive fluorescent dye, FluoZin-3 (Invitrogen). Cells were incubated with 5 μM FluoZin-3-AM in standard extracellular fluid (ECF) for 30 min at 37 °C, followed by de-esterification of the dye for another 30 min at room temperature (22–25 °C). The coverslips containing dye-loaded cells were held in a recording chamber placed on the stage of an inverted microscope (Eclipse TE2000-U; Nikon), and superfused with standard ECF at room temperature for at least 10 min prior to experiments. FluoZin-3 was excited at a wavelength of 490 nm, and emitted light was filtered with a 500–550-nm band pass filter. Zinc fluorescence was detected with a ×40 objective lens (Super Fluor ×40, numerical aperture = 0.90; Nikon) and a CCD camera (CoolSNAP ES2; Photometrics), using Imaging Workbench software (INDEC BioSystems). Fluorescence intensities (ΔF) were normalized to the resting values (F, average of five-data points recorded immediately before the change of solutions).

Solutions—For electrophysiology recording and zinc imaging, cells were superfused with a standard ECF containing (in mM) 140 NaCl, 5.4 KCl, 2 $CaCl_2$, 1 $MgCl_2$, 33 glucose, 20 HEPES (pH 7.4, adjusted with NaOH, and 320–335 mosmol with sucrose). For cortical neurons, MK-801 (10 μM; Sigma), 6-cyano-7-nitroquinoxaline-2,3-dione (20 μM; Sigma), and nimodipine (5 μM; Sigma) were included in the extracellular solutions to block potential zinc entry through NMDA and AMPA/kinate receptors, and VDCCs.

Oxygen-glucose Deprivation (OGD)—OGD was performed as described in our previous studies (30). The cultured cells were treated with glucose-free ECF containing (in mM) 140 NaCl, 5.4 KCl, 2 $CaCl_2$, 1 $MgCl_2$, 33 *N*-methyl-D-glucamine (or N-methyl-D-glucammonium at physiological pH), and 20 HEPES (pH 7.4, 320–335 mosmol), and then transferred to an anaerobic chamber containing 5% CO_2 and 95% N_2 atmosphere for 1 h. Cells were then washed with phosphate-buffered saline and placed in a normal cell culture incubator. All OGD experiments were carried out at 37 °C.

Propidium Iodide (PI) Staining and Analysis of Cell Injury—Cortical neurons were cultured on etched coverslips (Bellco Biotechnology) for monitoring the same cells before and after treatments. Three days after transfection, cells were treated with the indicated conditions for 1 h and then incubated in normal culture medium for 23 h. PI was added to the culture medium to a final concentration of 5 μg/ml. Images of the eGFP-positive cells were taken with the same fluorescent

microscope used for zinc imaging. PI-positive cells were regarded as injured cells. PI was excited at a wavelength of 540 nm, and emitted light was filtered with a 550–660-nm band pass filter. 6–20 cells were evaluated in each culture, and 3–5 independent cultures were included for each group.

Electrophysiology—Whole cell patch clamp recordings were performed as described previously (22, 34). 3–4 days after transfection, cells were set on the stage of the microscope and continuously superfused with ECF at room temperature. Patch electrodes were fabricated from borosilicate capillary tubing of 1.5-mm diameter (WPI) using a Narishige PP-83 vertical puller (Narishige). The electrode resistance ranged from 3 to 4 megohms when filled with the intracellular solution. Membrane currents were recorded using an Axopatch 200B amplifier. Data were filtered at 2 kHz and digitized at 5 kHz using a Digidata 1322A data acquisition system (Molecular Devices). Pipettes were filled with a solution containing (in mM) 140 CsF, 11 EGTA, 5 tetraethylammonium chloride, and 10 HEPES (pH 7.3, adjusted with CsOH). A multibarrel perfusion system (SF-77B, Warner Instrument) was employed for rapid exchange of solutions.

Statistical Analysis—Data were expressed as mean ± S.E. Groups were compared using one-way analysis of variance followed by Dunnett's test or unpaired Student's *t* test as appropriate. $p < 0.05$ was regarded as statistically significant (*, $p < 0.05$; **, $p < 0.01$).

RESULTS

Activation of TRPM7 Channels Enhances Zinc Toxicity in Mouse Cortical Neuron—Functional TRPM7 channels are expressed in neuronal cells where they play important roles in both physiological and pathological conditions (24, 35). Also, zinc ions have been reported to permeate through TRPM7 channels in heterologous expression systems (25). However, whether TRPM7 channels play a role in neuronal zinc dynamics and zinc-mediated neurotoxicity has never been explored. Therefore, we first examined whether promoting the activation of these channels affects zinc-induced injury of cultured mouse cortical neurons. In all experiments, the blockers for NMDA receptors, AMPA/kinate receptors, and VDCCs were included in the extracellular solutions to eliminate the potential zinc entry through these pathways (see "Experimental Procedures"). When 30 μM zinc was added to the extracellular solution to mimic brain ischemia (12, 36, 37), mouse cortical neurons showed a slight increase of cell injury as demonstrated by morphological changes (Fig. 1*A*) and increased LDH release measured at 24 h after zinc incubation (Fig. 1*B*). This zinc-induced cell injury was, however, dramatically exacerbated by Ca^{2+}/Mg^{2+} removal (Fig. 1, *A* and *B*), a condition known to activate TRPM7 channels (22, 24, 28). These results suggest that activation of TRPM7 channels promotes zinc toxicity in native neurons. Consistent with an involvement of TRPM7 channels, addition of Gd^{3+} and 2-aminoethoxydiphenyl borate, nonspecific inhibitors of TRPM7 channels (22, 24, 25, 28, 34), both attenuated zinc-induced neuronal injury (Fig. 1*C*).

Activation of TRPM7 Channels Increases $[Zn^{2+}]_i$ in Neurons—We next examined whether altering the function of TRPM7 channels affects intracellular zinc accumulation in cultured

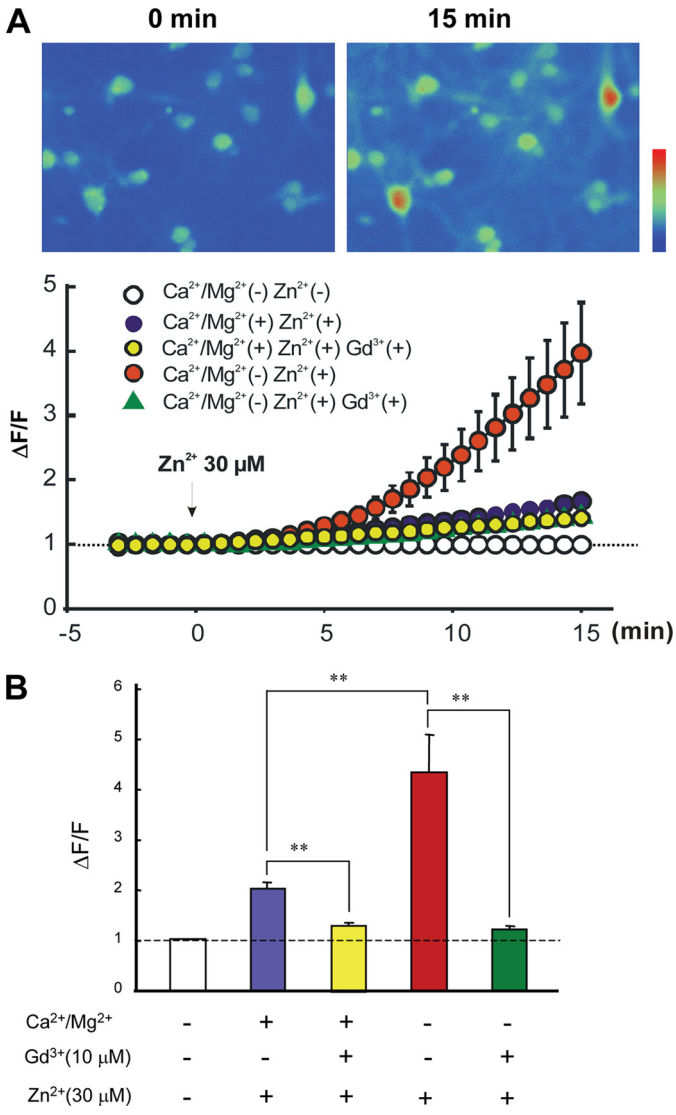

FIGURE 2. **Activation of TRPM7 channels induces an increase of $[Zn^{2+}]_i$ in neurons.** *A*, representative images and traces showing time-dependent changes of FluoZin-3 fluorescence in cultured mouse cortical neurons at the conditions indicated. Each trace represents an average fluorescent intensity from randomly selected 7–11 cells in an experiment. *B*, summary *bar graph* showing the normalized fluorescence intensity at the 15-min time point in the different conditions as indicated. $n = 20–54$ cells from three to six independent experiments. **, $p < 0.01$.

mouse cortical neurons using a zinc indicator FluoZin-3 (38). As shown in Fig. 2, *A* and *B*, application of 30 μM zinc in normal ECF slightly increased FluoZin-3 fluorescence intensity in cortical neurons (Fig. 2, *A* and *B*, *blue circle*). Activation of TRPM7 channels by removing Ca^{2+}/Mg^{2+} from the ECF induced a dramatic increase of FluoZin-3 fluorescence intensity (Fig. 2, *A* and *B*, *red circle*). Addition of Gd^{3+} (10 μM) dramatically attenuated the increase of FluoZin-3 fluorescence induced by Ca^{2+}/Mg^{2+} removal (Fig. 2, *A* and *B*, *green triangle*). In contrast, addition of Gd^{3+} did not affect the baseline FluoZin-3 fluorescence intensity ($n = 9$, supplemental Fig. S1*A*). Addition of (2-pyridylmethyl)ethylenediamine (TPEN), a high affinity zinc chelator (31), completely eliminated the increase of FluoZin-3 fluorescence intensity (supplemental Fig. S2*A*). Together, these data suggest that activation of TRPM7 channels can cause increases of $[Zn^{2+}]_i$ in mouse cortical neurons.

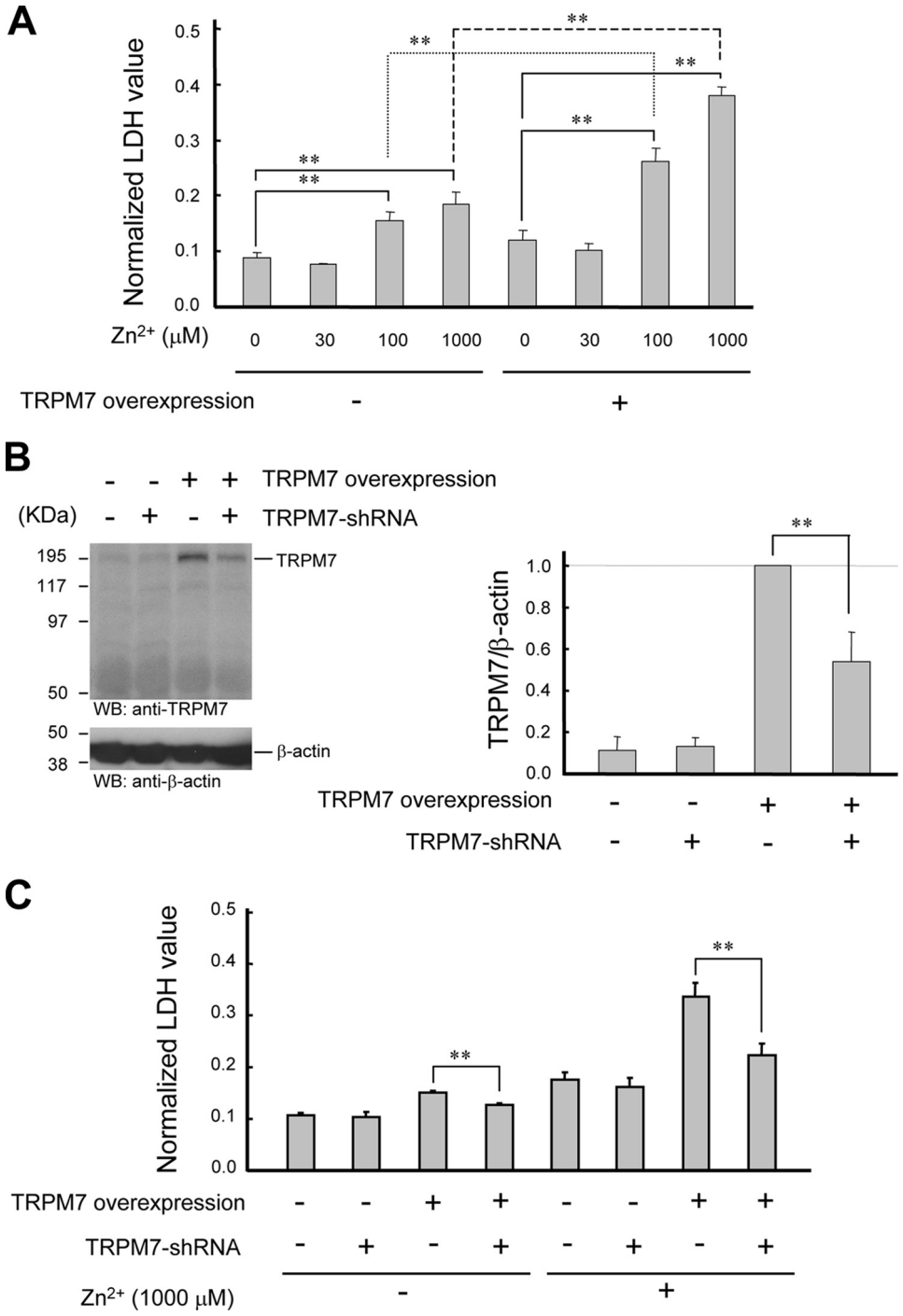

FIGURE 3. **Overexpression of TRPM7 channels renders HEK293 cells more sensitive to zinc toxicity.** *A*, HEK: TRPM7 cells were either untreated or treated with tetracycline for 2 days. Cells were then treated with the indicated concentrations of zinc for 1 h, incubated with culture medium for 23 h, followed by measurement of LDH release ($n = 9$). *B*, TRPM7(−) or (+) cells were transfected with the plasmid-based TRPM7-shRNA or mock vector, then either left untreated or treated with tetracycline for 2 days. TRPM7 protein levels were examined by immunoblotting using an antibody for TRPM7 (*upper*). Protein loading was monitored by immunoblotting using an antibody for β-actin (*lower*) ($n = 3$). *C*, TRPM7(−) or (+) cells were transfected with the plasmid-based TRPM7-shRNA or mock vector, then treated with or without zinc as indicated ($n = 8$). **, $p < 0.01$. *WB*, Western blot.

with inducible expression of TRPM7 channels (19, 22). In the absence of induced expression of TRPM7 channels (TRPM7(−) cells), incubation of HEK293 cells with 30 μM zinc for 1 h did not induce an increase of LDH release, although incubation with higher concentrations of zinc (100–1000 μM) did induce a significant increase of LDH release (Fig. 3*A*). However, when overexpression of the TRPM7 channel was induced by adding tetracycline (TRPM7(+) cells), incubation of HEK293 cells with zinc induced a greater increase of LDH release, suggesting that increased expression of TRPM7 channels exacerbates zinc-induced cell damage.

To confirm that the enhancement of zinc-mediated cell injury was indeed due to TRPM7 overexpression, RNA interference was employed to silence TRPM7 gene expression. Transfection of TRPM7(+) cells with TRPM7-shRNA reduced the TRPM7 protein level by ~50% at 48 h post-induction, as compared with cells transfected with a mock vector (Fig. 3*B*). This reduction in the protein level of TRPM7 was accompanied by a significant attenuation of zinc-induced LDH release (Fig. 3*C*), further supporting a role of TRPM7 channels in zinc-induced injury of HEK293 cells. In this experiment, a high concentration of zinc (1000 μM) was used to induce more cell death, which allows for easier detection of the reduction of cell injury by TRPM7-shRNA treatment.

TRPM7 Overexpression Increases $[Zn^{2+}]_i$ in HEK293 Cells—To determine whether changes of TRPM7 expression affect $[Zn^{2+}]_i$, zinc imaging was performed in HEK293 cells. As shown in Fig. 4, *A* and *B*, when 30 μM zinc was added to the extracellular solution, FluoZin-3 intensity gradually increased in both TRPM7(+) and TRPM7(−) cells. However, TRPM7(+) cells showed a much steeper increment in FluoZin-3 intensity than that of TRPM7(−) cells (Fig. 4*B*). Consistent with an involvement of TRPM7 activation, the increase of FluoZin-3 intensity in TRPM7(+) cells was largely attenuated by Gd^{3+} in a dose-dependent manner. Addition of Gd^{3+} did not affect the base-

Overexpression of TRPM7 Channels Enhances Zinc Toxicity in HEK293 Cells—To provide further evidence supporting the contribution of TRPM7 channels to zinc toxicity, we investigated if changing the expression levels of TRPM7 channels influences the zinc-mediated cell injury. We used HEK293 cells

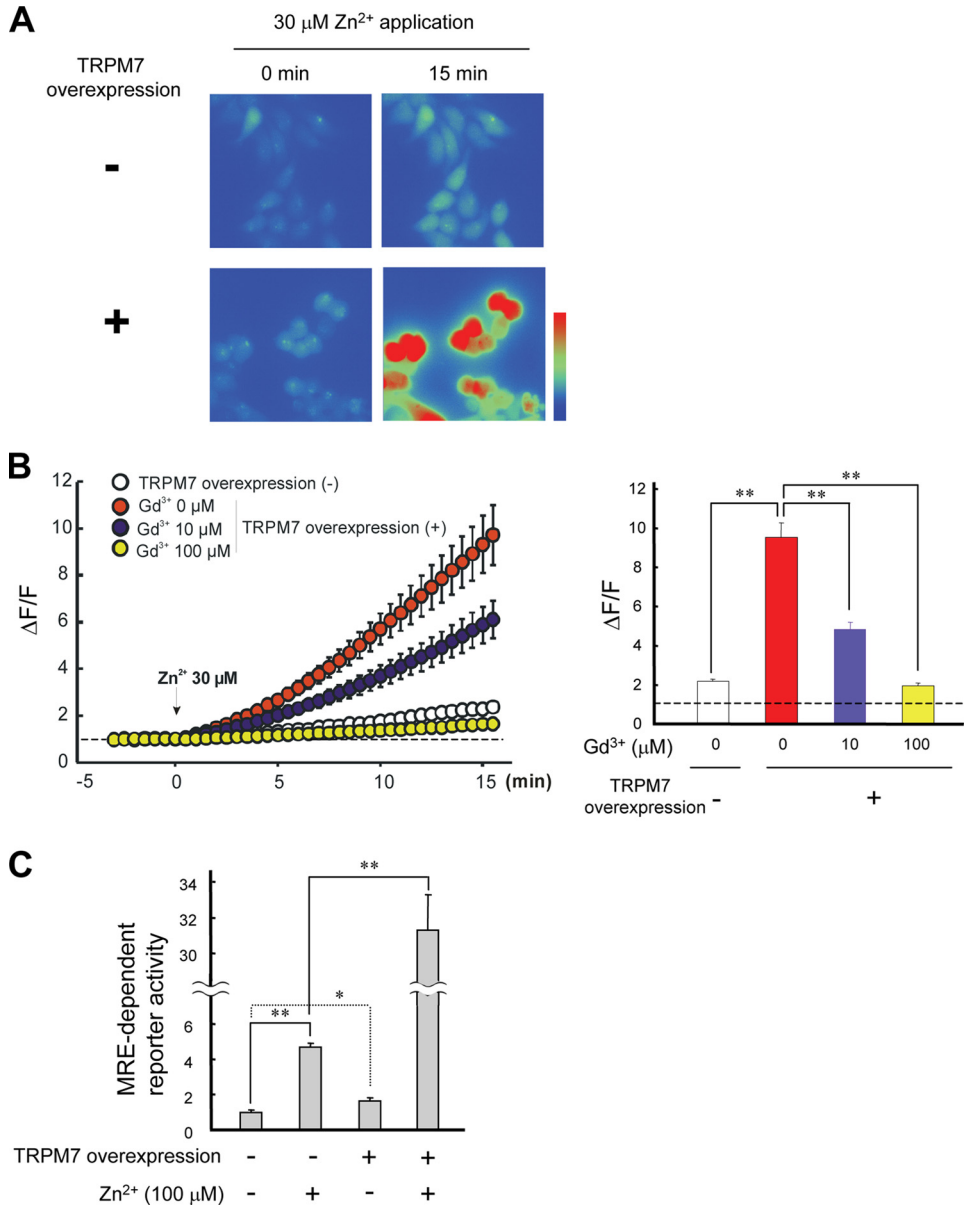

FIGURE 4. **Overexpression of TRPM7 channels increases intracellular zinc accumulation in HEK293 cells.** *A*, example images showing time-dependent changes of FluoZin-3 fluorescence in HEK293 cells either with or without TRPM7 overexpression. Cells were either untreated (*upper*) or treated with tetracycline (*lower*) for 2 days, incubated with FluoZin-3, and monitored on a fluorescence microscope. *B*, time-dependent increase of zinc fluorescence in HEK293 cells with or without TRPM7 overexpression, in the presence of different concentrations of Gd^{3+}. Each trace represents an average fluorescent intensity from randomly selected 8–16 cells in an experiment. The *bar graph* summarizes changes in zinc fluorescence at the 15-min time point. $n = 30–40$ cells from three independent experiments. *C*, effect of TRPM7 expression on zinc-induced MRE-dependent reporter activity. Cells were co-transfected with $p(MREa)_6$-Luc, a firefly luciferase reporter plasmid containing six tandem repeats of MRE, and pRL-TK, a control *Renilla* luciferase reporter plasmid. 2 h after transfection, TRPM7 expression was uninduced or induced by adding tetracycline. 40 h after transfection, cells were either untreated or treated with 100 μM zinc for 8 h before being harvested. For each condition, the ratio of firefly luciferase activity to *Renilla* luciferase activity was calculated ($n = 5$). *, $p < 0.05$; **, $p < 0.01$.

line intensity of FluoZin-3 fluorescence in the absence of added zinc ($n = 17$, supplemental Fig. S1*B*). Similar to neuronal cells, the increment of FluoZin-3 fluorescence intensity in TRPM7(+) cells was completely eliminated by the addition of TPEN (supplemental Fig. S2*B*). These results suggest that the level of $[Zn^{2+}]_i$ is largely determined by the level of TRPM7 channel expression.

To provide additional biochemical evidence that TRPM7 channels play an important role in determining the level of $[Zn^{2+}]_i$, we performed a reporter gene assay, in which a metal regulatory element (MRE) was involved upstream of firefly luciferase. MREs are known to be activated by binding metal-regulatory transcription factors in the presence of heavy metals such as zinc (32, 39). Thus, by measuring the MRE-dependent reporter activity, intracellular zinc levels can be indirectly evaluated (32, 39). As shown in Fig. 4*C*, TRPM7(+) cells were dramatically more responsive to zinc application than TRPM7(−) cells, suggesting a higher intracellular zinc level in TRPM7(+) cells. In addition to zinc application, TRPM7(+) cells also showed a higher baseline reporter activity (Fig. 4*C*), consistent with a higher basal level of $[Zn^{2+}]_i$ in these cells. A zinc-induced increase of reporter activity was also blocked by the addition of TPEN (supplemental Fig. S3).

Zinc Accumulation in Neurons Is Attenuated by TRPM7-shRNA—To further test our hypothesis that TRPM7 channels contribute to zinc accumulation in neurons, TRPM7-shRNA/eGFP was used to determine whether knocking down the expression of TRPM7 channels reduces the $[Zn^{2+}]_i$. As shown in Fig. 5*A*, cells transfected with TRPM7-shRNA/eGFP for 3–4 days significantly reduced the density of TRPM7-like current activated by Ca^{2+}/Mg^{2+} removal (28), as compared with cells transfected with control/eGFP. TRPM7-like currents in both control/eGFP and TRPM7-shRNA/eGFP-transfected cells were attenuated by 10 μM Gd^{3+}, suggesting that they were carried by TRPM7 channels. However, the difference between the current before Gd^{3+} and the current after Gd^{3+} is smaller in TRPM7-shRNA/eGFP-transfected cells, indicating suppression of the TRPM7 current by TRPM7-shRNA (Fig. 5*A*, *panel b*). In control/eGFP-transfected neurons, addition of 10 μM Gd^{3+} reduced the current density from 5.7 ± 1.1 to 2.0 ± 0.5 pA/pF ($n = 5$). In TRPM7-shRNA/eGFP-transfected cells, addition of 10 μM Gd^{3+} reduced the current density from 2.9 ± 0.6 to 1.4 ± 0.3 pA/pF ($n = 6$). The difference between the Gd^{3+}-sensitive current in mock-transfected cells and TRPM7-shRNA-transfected cells (3.7 *versus* 1.5 pA/pF) was statistically

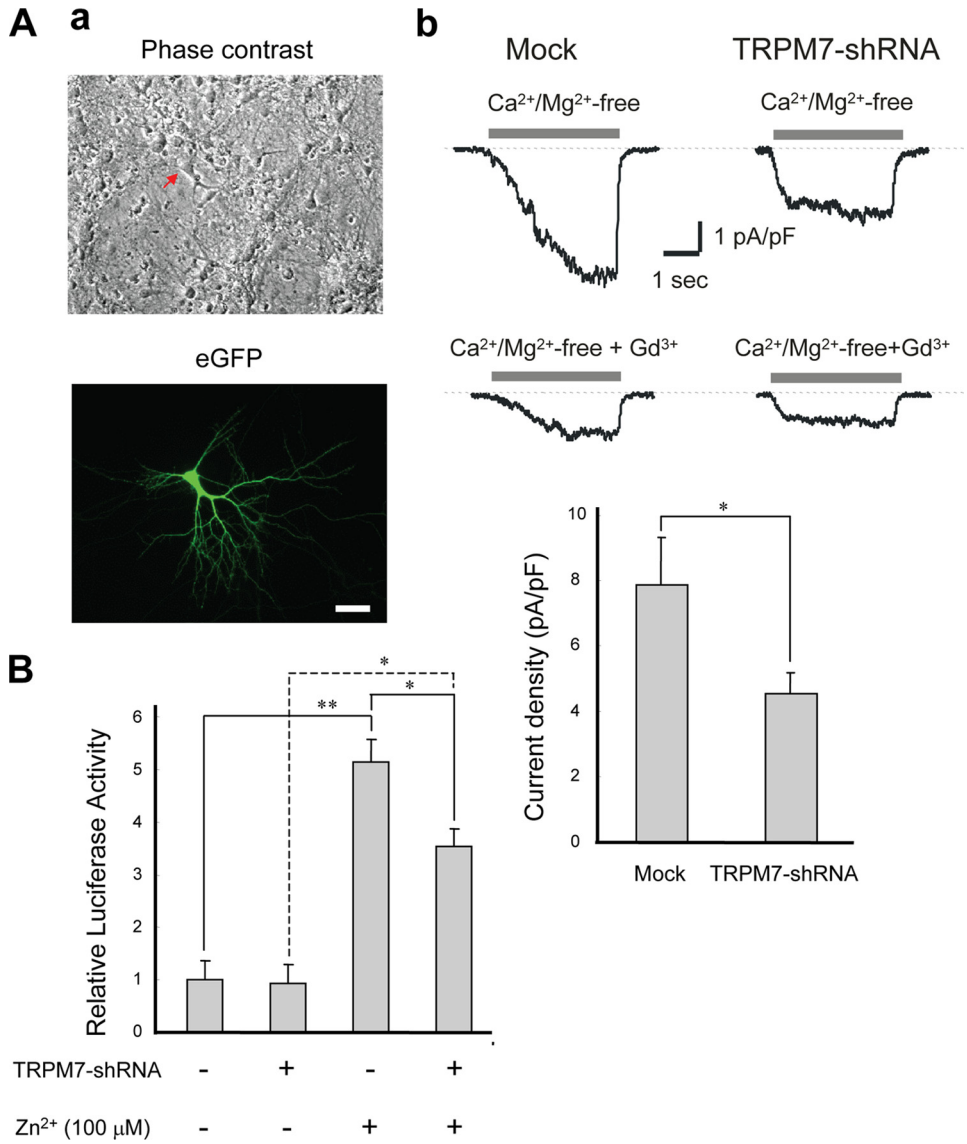

FIGURE 5. **Knockdown of TRPM7 channels with TRPM7-shRNA reduces TRPM7-like current and intracellular zinc concentration in mouse cortical neurons.** *A*, *a*, representative phase-contrast and fluorescent images of cortical neurons transfected with TRPM7-shRNA/eGFP. *Scale bar*, 50 μm. *b*, *upper panel*, representative traces showing TRPM7-like currents activated by Ca^{2+}/Mg^{2+} removal in cortical neurons transfected with mock vector (*left*) or TRPM7-shRNA (*right*). *b*, *lower panel*, summary *bar graph* showing the density of the TRPM7-like current in mouse cortical neurons transfected with control/eGFP ($n = 18$) and TRPM7-shRNA/eGFP ($n = 17$). The currents in both control/eGFP and TRPM7-shRNA/eGFP-transfected cells were inhibited by Gd^{3+} ($n = 4–5$), suggesting that they were mediated by TRPM7 channels. *B*, transfection of mouse cortical neurons with TRPM7-shRNA reduced intracellular zinc concentration as demonstrated by reduced luciferase activity. Cells were co-transfected with $p(MREa)_6$-Luc, pRL-TK, and a plasmid for either TRPM7-shRNA or control. 3 days after transfection, the cells were untreated or treated with 100 μM zinc for 8 h before being harvested. For each condition, the ratio of firefly luciferase activity to *Renilla* luciferase activity was calculated ($n = 8$). *, $p < 0.05$; **, $p < 0.01$.

significant ($p < 0.05$). We also examined the effect of shRNA on TRPM7 expression in neurons with immunocytochemistry. However, despite three different antibodies used, we were unable to obtain high quality TRPM7 immunostaining of cultured mouse cortical neurons. The overall staining of TRPM7 is weak in these neurons (not shown), making the quantitative comparison between control and TRPM7-shRNA-transfected cells unreliable.

Similar to the TRPM7-like current, silencing TRPM7 with TRPM7-shRNA significantly reduced the $[Zn^{2+}]_i$ in neurons as demonstrated by reduced MRE-dependent reporter activity (Fig. 5*B*). These results strongly suggest that TRPM7 channels play an important role in zinc accumulation in mouse cortical neurons.

Zinc-induced Neuronal Injury Is Attenuated by TRPM7-shRNA—To determine whether TRPM7 channels are involved in zinc-mediated neurotoxicity, the degree of zinc-induced injury of cultured mouse cortical neurons grown on etched coverslips was compared between TRPM7-shRNA/eGFP-transfected and control/eGFP-transfected cells. eGFP-positive neurons were recorded before and 24 h after a 1-h incubation with 30 μM zinc. As shown in Fig. 6, *A* and *B*, incubation of control/eGFP neurons with 30 μM zinc induced ~50% of cell death. However, the same treatment induced less than 30% injury of neurons transfected with TRPM7-shRNA/eGFP (Fig. 6, *A* and *B*). Similar to control/eGFP-transfected cells, 1 h incubation with 30 μM zinc induced ~50% of cell death in eGFP-negative cells. Thus, TRPM7 channels play an important role in zinc-induced injury of mouse cortical neurons.

TRPM7 Channels Mediate Zinc Toxicity under OGD Conditions—Finally, we determined whether TRPM7-mediated zinc toxicity is also involved in the OGD condition, an *in vitro* model of ischemia. Consistent with our previous studies (24), 1-h OGD, in the presence of the blockers of glutamate receptors and VDCCs, did not induce much damage to neurons. However, when 30 μM zinc was added, cell injury was dramatically increased (Fig. 7*A*). This damage was inhibited by Gd^{3+}, suggesting the involvement of TRPM7 channels. Further supporting this claim, TRPM7-shRNA/eGFP-tranfected cells were resistant to injury by zinc-OGD compared with control/eGFP-transfected cells (Fig. 7, *B* and *C*). Thus, TRPM7 is involved in zinc toxicity under ischemic conditions.

DISCUSSION

The significance of zinc homeostasis in normal brain function and in brain pathology has been increasingly recognized (8, 9, 12, 40, 41). The role of zinc in neuronal cell death associated with various neurological disorders, for example, has been studied. In ischemic conditions, it has been reported that extra-

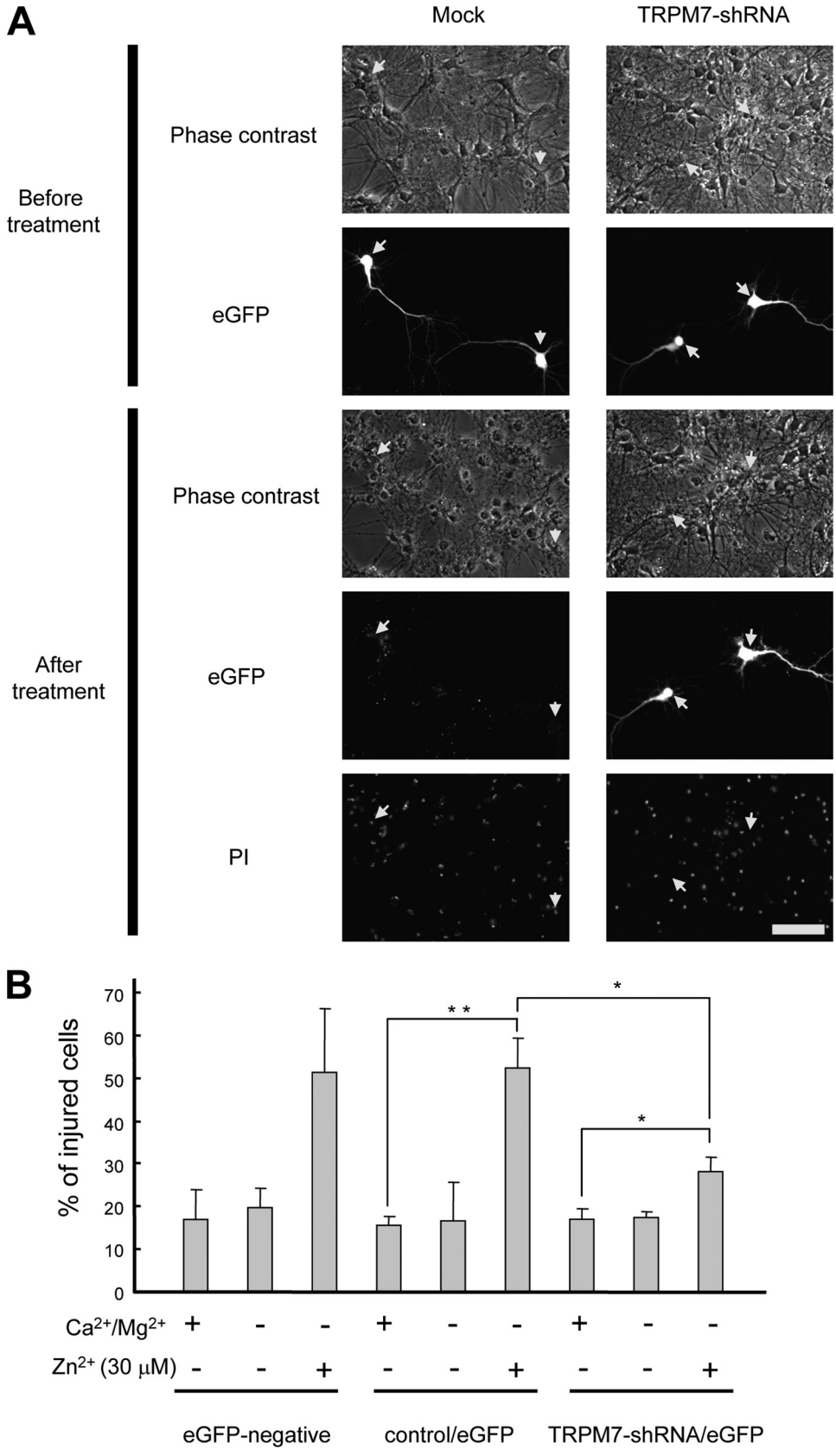

FIGURE 6. **Silencing TRPM7 reduces TRPM7-mediated zinc toxicity in mouse cortical neurons.** *A*, neurons were transfected with a plasmid expressing either control/eGFP or TRPM7-shRNA/eGFP for 3 days. They were then treated with Ca^{2+}/Mg^{2+}-free ECF with 30 μM zinc for 1 h, followed by a 23-h incubation with normal culture medium. *Scale bar*, 50 μm. *B*, summary *bar graph* showing percentage of injured cells in the indicated groups. *, $p < 0.05$; **, $p < 0.01$.

cellular chelation of zinc reduces cell injury (9, 12, 42). In seizure conditions, zinc acts either as an anticonvulsant or proconvulsant depending on the type of seizure (12, 43, 44). In addition, the potential involvement of zinc in the pathology of Alzheimer disease has been documented. For example, it has been shown that the amyloid plaque is highly enriched with chelatable zinc and the expression level of ZnTs is altered in patients with Alzheimer disease (12, 40, 45, 46). Although both extra- and intracellular zinc are tightly regulated at low levels under physiological conditions, they change dramatically under pathological conditions (12, 40). Levels of extracellular zinc at tens of micromolar, for example, have been reported following brain ischemia (12, 36, 37). The increased level of extracellular zinc is accompanied by a dramatic increase in intracellular zinc and resultant neurotoxicity, although the exact zinc entry pathways have not been clearly delineated.

Recent studies have demonstrated that some ion channels and transporters, *e.g.* VDCCs and glutamate receptor-gated channels, are zinc permeable (16, 17). Activation of these channels is therefore expected to play a role in zinc homeostasis and toxicity. Unfortunately, clinical trials showed little effectiveness of their blockers in protecting the ischemic brain (3). Searching for additional pathways involved in intracellular zinc accumulation and toxicity may help for establishing new and effective neuroprotective strategies. In this study, we provided strong evidence suggesting that TRPM7 is an important player for intracellular zinc accumulation and zinc-induced neurotoxicity. Based on their non-desensitizing nature and potentiation by acidosis (see below), TRPM7 channels likely play an important role in zinc accumulation associated with ischemic neuronal injury.

Studies by Monteilth-Zoller *et al.* (25) first indicated zinc permeation through recombinant TRPM7

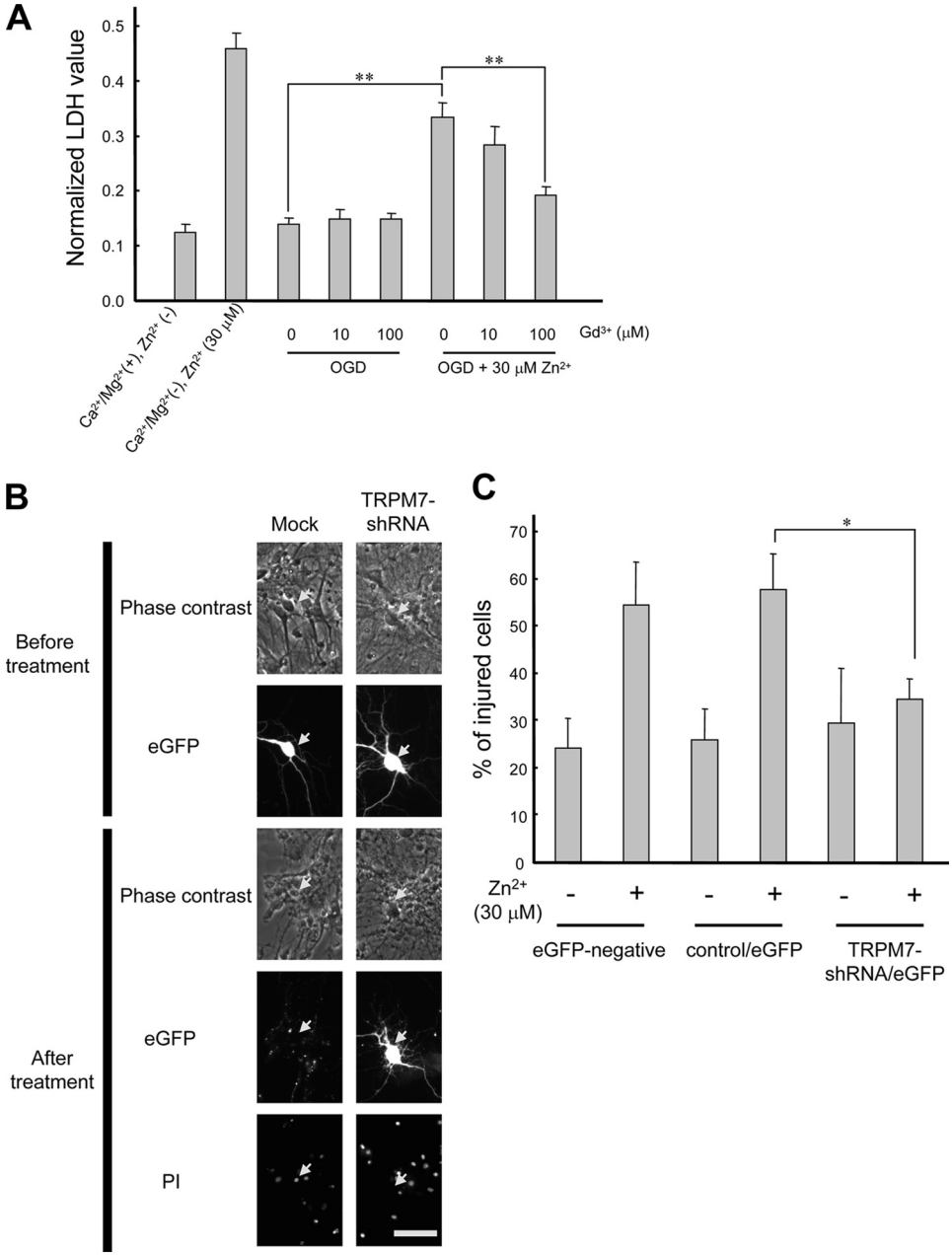

FIGURE 7. **TRPM7 channels mediate zinc toxicity of neurons under ischemic condition.** *A*, cells were incubated under the OGD condition in the absence or presence of 30 μM zinc for 1 h, followed by incubation with normal culture medium for 23 h. Cell injury was quantified with LDH release ($n = 16$). *B*, neurons were transfected with a plasmid expressing either control/eGFP or TRPM7-shRNA/eGFP for 3 days. They were then treated with or without 30 μM zinc under the OGD condition for 1 h, followed by a 23-h incubation with normal culture medium. *Scale bar*, 50 μm. *C*, summary *bar graph* showing percentage of injured cells in the indicated groups. *, $p < 0.05$; **, $p < 0.01$.

channels, using electrophysiological measurements. The studies were performed using millimolar concentrations of zinc, which are several orders of magnitude higher than the physiological/pathophysiological concentrations of zinc (25). In the present studies, we explored the role of native TRPM7 channels in intracellular zinc accumulation at physiological/pathological relevant concentrations (12), and more importantly, in zinc-induced neuronal injury.

Using fluorescent zinc imaging, we demonstrated direct increases in stimulated $[Zn^{2+}]_i$ in cortical neurons, and that this increase of $[Zn^{2+}]_i$ was suppressed by Gd^{3+}, a commonly used nonspecific blocker of TRPM7 channels. We then demonstrated that activation of TRPM7 channels augmented zinc-induced cell injury. In contrast, knockdown of the expression of TRPM7 channels with TRPM7-shRNA, or blocking the function of TRPM7 channels with Gd^{3+}, both reduced zinc-mediated cell injury. Interestingly, cell injury caused by Ca^{2+}/Mg^{2+} removal in the absence of added zinc was not affected by TPEN (data not shown), indicating that residual zinc in the extracellular solution, which is in the 20–50 nM range (26), is not responsible for cell injury. Therefore, the underlying mechanism for this baseline cell injury is not clear at present. We suspect that increased Na^+ entry through TRPM7 channels could be partially responsible for increased neuronal toxicity upon removing Ca^{2+}/Mg^{2+} in the absence of added zinc. Similar to cortical neurons, we show that increased TRPM7 expression is associated with elevated $[Zn^{2+}]_i$ in HEK293 cells and zinc-induced cell injury. This zinc-mediated cell toxicity was also inhibited by TRPM7-shRNA.

Activation of TRPM7 channels has been shown to contribute to Ca^{2+} toxicity in neurons (24, 28). Using Ca^{2+}/Mg^{2+} removal to activate TRPM7 channels eliminates Ca^{2+} entry and thus Ca^{2+}-dependent toxicity through these channels. Under this condition, zinc entry through TRPM7 channels can still induce dramatic cell injury. Therefore, targeting Ca^{2+} alone may not be sufficient to protect neurons from injury.

Following brain ischemia, increased production of reactive oxygen species, reduced concentration of extracellular Ca^{2+} ($[Ca^{2+}]_o$), and the change of cellular ATP/ADP content, all facilitate the opening of TRPM7 channels resulting in toxic Ca^{2+} loading (24, 47, 48). Compared with other Ca^{2+}-permeable cation channels involved in ischemic Ca^{2+} loading, *e.g.* NMDA channels, VDCCs, and recently identified acid-sensing ion channels, TRPM7 channels do not show clear desensitization over time (see Fig. 5*A*, for example), meaning that the channels remain open whenever the activators (*e.g.* reactive oxygen species, reduced $[Ca^{2+}]_o$, and acidosis, see below) are present. This characteristic likely makes the TRPM7 channels

unique and one of the important players in ischemic neuronal injury.

Although Ca^{2+} entry through TRPM7 channels plays an important role in neuronal injury, our findings suggest that zinc entry through these channels could be equally important in TRPM7-mediated neuronal injury. It is worth mentioning that $[Ca^{2+}]_o$ decreases dramatically during ischemia to as low as 0.1 mM (49). This reduction of $[Ca^{2+}]_o$ should dramatically reduce the driving force for Ca^{2+} thus limiting Ca^{2+} entry, *e.g.* through TRPM7 channels. In contrast to the reduction of $[Ca^{2+}]_o$, extracellular zinc concentration increases following brain ischemia (50–52). This should facilitate the entry of zinc through zinc-permeable channels, thus promoting the zinc-mediated neuronal injury.

During ischemia, a significant drop in brain pH also takes place. A reduced pH is known to inhibit the activity of NMDA receptors and VDCCs (53–55), two major zinc permeable channels (16). Thus, zinc entry through these channels would be limited. In contrast, acidosis has been shown to potentiate, rather than inhibit, the activation of TRPM7 channels (48). Based on all these factors, TRPM7 channels may represent an important zinc entry pathway in the ischemic brain. Therefore, targeting these channels could be a novel neuroprotective strategy for stroke patients, particularly following the failure of clinical trials using glutamate antagonists (3).

Acknowledgments—We thank Dr. J. Miyazaki for providing pCAGGS-eGFP, Dr. C. Seguin for providing p(MREa)$_6$-Luc, and Dr. A. Scharenberg (University of Washington) for providing HEK293 cells with inducible expression of TRPM7.

REFERENCES

1. Choi, D. W. (1988) *Trends Neurosci.* **11,** 465–469
2. Birmingham, K. (2002) *Nat. Med.* **8,** 5
3. Ikonomidou, C., and Turski, L. (2002) *Lancet Neurol.* **1,** 383–386
4. Cheng, C., and Reynolds, I. J. (1998) *J. Neurochem.* **71,** 2401–2410
5. Stork, C. J., and Li, Y. V. (2006) *J. Neurosci.* **26,** 10430–10437
6. Grynkiewicz, G., Poenie, M., and Tsien, R. Y. (1985) *J. Biol. Chem.* **260,** 3440–3450
7. Simons, T. J. (1993) *J. Biochem. Biophys. Methods* **270,** 25–37
8. Calderone, A., Jover, T., Mashiko, T., Noh, K. M., Tanaka, H., Bennett, M. V., and Zukin, R. S. (2004) *J. Neurosci.* **24,** 9903–9913
9. Koh, J. Y., Suh, S. W., Gwag, B. J., He, Y. Y., Hsu, C. Y., and Choi, D. W. (1996) *Science* **272,** 1013–1016
10. Beyersmann, D., and Haase, H. (2001) *Biometals* **14,** 331–341
11. Cuajungco, M. P., and Lees, G. J. (1997) *Neurobiol. Dis.* **4,** 137–169
12. Frederickson, C. J., Koh, J. Y., and Bush, A. I. (2005) *Nat. Rev. Neurosci.* **6,** 449–462
13. Palm, R., Sjöström, R., and Hallmans, G. (1983) *Clin. Chem.* **29,** 486–491
14. Liuzzi, J. P., and Cousins, R. J. (2004) *Annu. Rev. Nutr.* **24,** 151–172
15. Lichten, L. A., and Cousins, R. J. (2009) *Annu. Rev. Nutr.* **29,** 153–176
16. Sensi, S. L., Canzoniero, L. M., Yu, S. P., Ying, H. S., Koh, J. Y., Kerchner, G. A., and Choi, D. W. (1997) *J. Neurosci.* **17,** 9554–9564
17. Canzoniero, L. M., Turetsky, D. M., and Choi, D. W. (1999) *J. Neurosci.* **19,** RC31
18. Clapham, D. E. (2003) *Nature* **426,** 517–524
19. Nadler, M. J., Hermosura, M. C., Inabe, K., Perraud, A. L., Zhu, Q., Stokes, A. J., Kurosaki, T., Kinet, J. P., Penner, R., Scharenberg, A. M., and Fleig, A. (2001) *Nature* **411,** 590–595
20. Runnels, L. W., Yue, L., and Clapham, D. E. (2001) *Science* **291,** 1043–1047
21. Jin, J., Desai, B. N., Navarro, B., Donovan, A., Andrews, N. C., and Clapham, D. E. (2008) *Science* **322,** 756–760
22. Jiang, J., Li, M. H., Inoue, K., Chu, X. P., Seeds, J., and Xiong, Z. G. (2007) *Cancer Res.* **67,** 10929–10938
23. Schmitz, C., Perraud, A. L., Johnson, C. O., Inabe, K., Smith, M. K., Penner, R., Kurosaki, T., Fleig, A., and Scharenberg, A. M. (2003) *Cell* **114,** 191–200
24. Aarts, M., Iihara, K., Wei, W. L., Xiong, Z. G., Arundine, M., Cerwinski, W., MacDonald, J. F., and Tymianski, M. (2003) *Cell* **115,** 863–877
25. Monteilh-Zoller, M. K., Hermosura, M. C., Nadler, M. J., Scharenberg, A. M., Penner, R., and Fleig, A. (2003) *J. Gen. Physiol.* **121,** 49–60
26. Chu, X. P., Wemmie, J. A., Wang, W. Z., Zhu, X. M., Saugstad, J. A., Price, M. P., Simon, R. P., and Xiong, Z. G. (2004) *J. Neurosci.* **24,** 8678–8689
27. Inoue, K., Ueno, S., and Fukuda, A. (2004) *FEBS Lett.* **564,** 131–135
28. Wei, W. L., Sun, H. S., Olah, M. E., Sun, X., Czerwinska, E., Czerwinski, W., Mori, Y., Orser, B. A., Xiong, Z. G., Jackson, M. F., Tymianski, M., and MacDonald, J. F. (2007) *Proc. Natl. Acad. Sci. U.S.A.* **104,** 16323–16328
29. Niwa, H., Yamamura, K., and Miyazaki, J. (1991) *Gene* **108,** 193–199
30. Xiong, Z. G., Zhu, X. M., Chu, X. P., Minami, M., Hey, J., Wei, W. L., MacDonald, J. F., Wemmie, J. A., Price, M. P., Welsh, M. J., and Simon, R. P. (2004) *Cell* **118,** 687–698
31. Hey, J. G., Chu, X. P., Seeds, J., Simon, R. P., and Xiong, Z. G. (2007) *Stroke* **38,** 670–673
32. LaRochelle, O., Gagné, V., Charron, J., Soh, J. W., and Séguin, C. (2001) *J. Biol. Chem.* **276,** 41879–41888
33. Inoue, K., Zama, T., Kamimoto, T., Aoki, R., Ikeda, Y., Kimura, H., and Hagiwara, M. (2004) *Genes Cells* **9,** 59–70
34. Inoue, K., and Xiong, Z. G. (2009) *Cardiovasc. Res.* **83,** 547–557
35. Krapivinsky, G., Mochida, S., Krapivinsky, L., Cibulsky, S. M., and Clapham, D. E. (2006) *Neuron* **52,** 485–496
36. Li, Y., Hough, C. J., Suh, S. W., Sarvey, J. M., and Frederickson, C. J. (2001) *J. Neurophysiol.* **86,** 2597–2604
37. Ueno, S., Tsukamoto, M., Hirano, T., Kikuchi, K., Yamada, M. K., Nishiyama, N., Nagano, T., Matsuki, N., and Ikegaya, Y. (2002) *J. Cell Biol.* **158,** 215–220
38. Gee, K. R., Zhou, Z. L., Qian, W. J., and Kennedy, R. (2002) *J. Am. Chem. Soc.* **124,** 776–778
39. Andrews, G. K. (2000) *Biochem. Pharmacol.* **59,** 95–104
40. Capasso, M., Jeng, J. M., Malavolta, M., Mocchegiani, E., and Sensi, S. L. (2005) *J. Alzheimers Dis.* **8,** 93–108
41. Bossy-Wetzel, E., Talantova, M. V., Lee, W. D., Schölzke, M. N., Harrop, A., Mathews, E., Götz, T., Han, J., Ellisman, M. H., Perkins, G. A., and Lipton, S. A. (2004) *Neuron* **41,** 351–365
42. Tønder, N., Johansen, F. F., Frederickson, C. J., Zimmer, J., and Diemer, N. H. (1990) *Neurosci. Lett.* **109,** 247–252
43. Cole, T. B., Robbins, C. A., Wenzel, H. J., Schwartzkroin, P. A., and Palmiter, R. D. (2000) *Epilepsy Res.* **39,** 153–169
44. Rayatzadeh, H., Nouri, M., Ghasemi, M., Kebriaeezadeh, A., Mehr, S. E., and Dehpour, A. R. (2009) *Seizure* **18,** 51–56
45. Lovell, M. A., Smith, J. L., Xiong, S., and Markesbery, W. R. (2005) *Neurotox. Res.* **7,** 265–271
46. Smith, J. L., Xiong, S., Markesbery, W. R., and Lovell, M. A. (2006) *Neuroscience* **140,** 879–888
47. Demeuse, P., Penner, R., and Fleig, A. (2006) *J. Gen. Physiol.* **127,** 421–434
48. Jiang, J., Li, M., and Yue, L. (2005) *J. Gen. Physiol.* **126,** 137–150
49. Hansen, A. J., and Zeuthen, T. (1981) *Acta Physiol. Scand.* **113,** 437–445
50. Wei, G., Hough, C. J., Li, Y., and Sarvey, J. M. (2004) *Neuroscience* **125,** 867–877
51. Kitamura, Y., Iida, Y., Abe, J., Mifune, M., Kasuya, F., Ohta, M., Igarashi, K., Saito, Y., and Saji, H. (2006) *Brain Res. Bull.* **69,** 622–625
52. Frederickson, C. J., Giblin, L. J., Krezel, A., McAdoo, D. J., Mueller, R. N., Zeng, Y., Balaji, R. V., Masalha, R., Thompson, R. B., Fierke, C. A., Sarvey, J. M., de Valdenebro, M., Prough, D. S., and Zornow, M. H. (2006) *Exp. Neurol.* **198,** 285–293
53. Traynelis, S. F., and Cull-Candy, S. G. (1990) *Nature* **345,** 347–350
54. Tang, C. M., Dichter, M., and Morad, M. (1990) *Proc. Natl. Acad. Sci. U.S.A.* **87,** 6445–6449
55. Tombaugh, G. C., and Somjen, G. G. (1996) *J. Physiol.* **493,** 719–732